

Origin of Spectral Hardening of Secondary Cosmic-Ray Nuclei

Norita Kawanaka^{1,2*} and Shiu-Hang Lee¹

¹*Department of Astronomy, Graduate School of Science, Kyoto University, Kitashirakawa Oiwake-cho, Sakyo-ku, Kyoto, 606-8502, Japan*

²*Hakubi Center, Kyoto University, Yoshida-honmachi, Sakyo-ku, Kyoto, 606-8501, Japan*

26 February 2021

ABSTRACT

We discuss the acceleration and escape of secondary cosmic-ray (CR) nuclei, such as lithium, beryllium and boron, produced by spallation of primary CR nuclei like carbon, nitrogen, and oxygen accelerated at the shock in supernova remnants (SNRs) surrounded by the interstellar medium (ISM) or a circumstellar medium (CSM). We take into account the energy-dependent escape of CR particles from the SNR shocks, which is supported by gamma-ray observations of SNRs, to calculate the spectra of primary and secondary CR nuclei running away into the ambient medium. We find that if the SNR is surrounded by a CSM with a wind-like density distribution (i.e., $n_{\text{CSM}} \propto r^{-2}$), the spectra of the escaping secondary nuclei are harder than those of the escaping primary nuclei, while if the SNR is surrounded by a uniform ISM, the spectra of the escaping secondaries are always softer than those of the escaping primaries. Using this result, we show that if there was a past supernova surrounded by a dense wind-like CSM ($\sim 2.5 \times 10^{-3} M_{\odot} \text{ yr}^{-1}$) which happened $\sim 1.6 \times 10^5$ yr ago at a distance of ~ 1.6 kpc, we can simultaneously reproduce the spectral hardening of primary and secondary CRs above ~ 200 GV that have recently been reported by AMS-02.

Key words: acceleration of particles – cosmic rays – shock waves – supernova remnants

1 INTRODUCTION

Cosmic-ray (CR) secondary nuclei such as lithium, beryllium, and boron are considered to be produced via spallation of heavier nuclei such as carbon, nitrogen, and oxygen, which are mainly produced at Galactic supernova remnants (SNRs), during their propagation in the interstellar medium (ISM). The amount of secondary CR nuclei produced per primary nucleus is proportional to the grammage traversed by the primaries in the ISM. Therefore, the fluxes and rigidity dependence of secondary CRs are considered to be a probe of the propagation of CRs in our Galaxy. The boron-to-carbon (B/C) ratio has been measured up to \sim TeV per nucleon by AMS-02 (Aguilar et al. 2016b), and it has been shown that above the rigidity R of 65 GV the B/C ratio can be well fitted with a power law, $\propto R^{\Delta}$ with the index $\Delta \simeq -0.333$. This agrees well with what is expected from the Kolmogorov turbulence theory, in which Δ is asymptotically equal to $-1/3$ (Kolmogorov 1941), and therefore it is suggested that the spatial diffusion coefficient D as a function of rigidity is proportional to $R^{1/3}$. However, AMS-02 later reported that the spectra of CR lithium, beryllium, and boron deviate from a single power law above 200 GV in an identical way and that they harden even more than the primary CRs (Aguilar et al. 2018) which have already been known to harden at higher rigidities from measurements by PAMELA (Adriani et al. 2011), CREAM (Ahn et al. 2010), and AMS-02 (Aguilar et al. 2015a,b; Aguilar et al. 2017).

Several scenarios have been discussed to account for the deviation of the index of the secondary-to-primary ratio at high rigidities from what is expected from the diffusion coefficient in the bulk of the ISM, including the effect of

propagation in the Galaxy (Cowsik & Burch 2010; Tomassetti 2012; Cowsik et al. 2014; Cowsik & Madziwa-Nussinov 2016; Tomassetti 2015), re-acceleration of secondary CRs (Bresci et al. 2019; Yuan et al. 2020), contribution from different kinds of sources (Kawanaka & Yanagita 2018; Boschini et al. 2020; Niu 2020) and the effect of acceleration of secondary CRs in supernova remnants (SNRs) (Mertsch & Sarkar 2009; Ahlers et al. 2009; Kachelrieß & Ostapchenko 2013; Mertsch & Sarkar 2014; Cholis & Hooper 2014). These models are proposed mainly to explain the positron fraction measured by PAMELA and AMS-02 (Adriani et al. 2009; Aguilar et al. 2013), the antiproton-to-proton ratio measured by AMS-02 (Aguilar et al. 2016a), or the spectral hardening of proton and helium (Adriani et al. 2011; Aguilar et al. 2015a,b). Especially, in the last scenario, secondary CR nuclei are produced inside the SNRs via the spallation of primary CR nuclei being accelerated at the SNR shock, and are accelerated at the same shock. Since the spectra of secondary CR nuclei produced in this way are harder than that of primary CR nuclei, if their contributions are comparable to the background CR fluxes above a certain rigidity, the rigidity dependence of the secondary-to-primary ratio would deviate from what is expected from simple ISM diffusion. Very recently, Mertsch et al. (2020) performed a comprehensive study on this scenario by searching for the best fit parameters to account for the recent AMS-02 measurements of CR protons, helium, positrons, anti-protons, and primary/secondary nuclei. However, they discuss the spectra of secondary CRs that are shock-accelerated and advected to the downstream (i.e., inside the SNRs), and they do not consider the spectra of CRs escaping from the SNRs, which are what we observe.

In this paper we discuss the energy-dependent escape of primary and secondary CRs that are accelerated in the SNR shock,

* E-mail: norita@kusastro.kyoto-u.ac.jp

and predict their energy spectrum assuming that they come from a local SNR. The escape of CR particles from an SNR has been intensively investigated to interpret the observed CR spectra and the gamma-ray emission feature of SNRs interacting with molecular clouds (Ptuskin & Zirakashvili 2005; Reville et al. 2009; Gabici et al. 2009; Caprioli et al. 2010; Ohira et al. 2010, 2011, 2012, 2016; Ohira & Ioka 2011; Drury 2011; Kawanaka et al. 2011; Bell et al. 2013). If CRs escape the SNR in an energy-dependent way, the spectrum of escaping CRs would be steeper than that of CRs trapped inside the SNR (Ohira et al. 2010; Caprioli et al. 2010), which may account for the steepness of the observed CR spectral index. Therefore, it is worth investigating theoretically the production, acceleration, and escape of secondary CRs in an SNR, and comparing them with observational data. In this work, we consider CR acceleration in SNRs not only within a uniform ISM but also those surrounded by a dense circumstellar medium (CSM). Recent intense optical and near-infrared transient searches have revealed that many SNe show signs of strong interaction between their ejecta and the CSM surrounding them. There are various classes of CSM-interacting SNe: Type IIn, Ibn, Ia-CSM, type I superluminous SN, etc (for a comprehensive review, see Smith 2017). The origin of such dense CSM is still uncertain, but many observations indicate that their progenitors had expelled the stellar material shortly before their explosions, and the mass-loss rates estimated from their observational properties are up to $\sim 10^{-3} M_{\odot} \text{ yr}^{-1}$ (assuming their wind velocities are $\sim 100 \text{ km s}^{-1}$), continuing for decades (Moriya et al. 2014). The non-thermal emissions of photons or neutrinos due to the strong interactions between an SN ejecta and a dense CSM have been investigated in some studies (Murase et al. 2019; Wang et al. 2019; Matsuoka et al. 2019; Cristofari et al. 2020; Matsuoka & Maeda 2020), but the CR production and escape in such a system have not been discussed yet.

In Section 2, we describe our model of CR production inside a SNR surrounded by a CSM and energy-dependent escape of primary and secondary CRs. In Section 3 we solve the transport equations for primary and secondary CR nuclei to evaluate the spectra of the escaping CRs, compare them with observations, and discuss our results in light of stellar evolution scenarios. We conclude our work in Section 4.

2 MODEL

2.1 Energy-dependent Cosmic-ray Escape Scenario

Here we describe how CR particles accelerated at the SNR shock escape the source into the ISM depending on their energy, following Ohira et al. (2010). In the context of the diffusive shock acceleration (DSA) theory (Blandford & Eichler 1987), particles can go back and forth across the shock front and gain kinetic energy because they are scattered by the turbulent magnetic field around the shock. Especially, the turbulence in the upstream (i.e. the outside of the SNR shock) may be amplified by the streaming instability caused by the accelerating particles themselves (Bell 1978; Lucek & Bell 2000). Since the turbulence is generated only in the vicinity of the shock front, if accelerated particles have sufficiently high energy, they can escape the SNR into the far upstream region without being trapped by the turbulent magnetic field. Using the diffusion coefficient of accelerated particles as a function of their momentum $D(p)$, the shock velocity u_{sh} , and the distance from the shock beyond which the turbulence is negligible l , the escape condition for a particle accelerated at the shock can be described as

$$\frac{D(p)}{u_{\text{sh}}} \gtrsim l, \quad (1)$$

where the left hand side represents the diffusion length of a particle with momentum p . Zirakashvili & Ptuskin (2008) investigated the generation of magnetohydrodynamic (MHD) turbulence driven by the non-resonant streaming instability using numerical MHD calculations, and show that l should be the same order as the radius of the SNR, R_{sh} .

As a SNR evolves with time, the magnetic field around the shock decays and the speed of the SNR shell slows down. As a result, the escape condition Eq.(1) also evolves with time. Especially, if the diffusion length of a particle with a specific momentum increases faster than the SNR radius ($\sim l$), the required momentum of particles for escaping the SNR decreases with time. In other words, CR particles accelerated at the SNR shock can escape the SNR to far-upstream in an energy-dependent way. In the following subsections, we will evaluate the energy distribution of CR particles produced in a SNR taking into account the spallation of primary CRs, the production of secondary CRs, and their energy-dependent escape.

2.2 Primary and Secondary Cosmic-rays in the Supernova Remnant Shock

Here we present our formalism to derive the energy distributions of primary and secondary CRs produced in the SNR and their escaping fluxes as functions of time. In the following discussion, we focus on the CR nuclei of lithium, beryllium, boron, carbon, nitrogen, and oxygen. Among them, only oxygen is regarded as a pure primary element, and other lighter elements are partly or entirely produced via spallation of heavier nuclei during their propagation.

We assume that the CR particles can be regarded as test particles during DSA in a SNR. Letting the shock front be at $x = 0$, the stationary transport equation for the distribution functions of CR nuclei $f_i(x, p)$ (i represents the type of nuclei) in the shock rest frame is

$$u(x) \frac{\partial f_i}{\partial x} = \frac{\partial}{\partial x} \left[D_i(p) \frac{\partial f_i}{\partial x} \right] + \frac{p}{3} \frac{du}{dx} \frac{\partial f_i}{\partial p} - \Gamma_i f_i + q_i + u_- Q_i \delta(x) \delta(p - p_0), \quad (2)$$

where $u(x)$ is the fluid velocity, $D_i(p)$ is the diffusion coefficient for a nuclei of i with momentum p , Γ_i is the total spallation rate of a nuclei i (i.e. $\Gamma_i = \sum_{i>j} \Gamma_{i \rightarrow j}$), q_i is the source term due to the spallation of parent particles, and Q_i is the injection rate of a nuclei i at the shock front (the injection momentum is p_0). Considering that the kinetic energy per nucleon of a nucleus is conserved before and after the spallation, q_i is given by

$$4\pi p^2 \frac{dp}{d\varepsilon_k} q_i(p) = \sum_{i<j} \Gamma_{j \rightarrow i} N_j(\varepsilon_k), \quad (3)$$

where $N_j(\varepsilon_k) = 4\pi p^2 f_j(p) (dp_j/d\varepsilon_k)$ (p_j is the momentum of a nucleus j with kinetic energy of ε_k) is the kinetic energy distribution function of nuclei j , and $\Gamma_{j \rightarrow i}$ is the rate at which a nucleus i is produced via spallation of a heavier nucleus j . The fluid velocity is given by

$$u(x) = \begin{cases} u_- & (x < 0) \\ u_+ & (x > 0), \end{cases} \quad (4)$$

where $u_- = u_{\text{sh}}$ and $u_+ = u_{\text{sh}}/r$ are constants, and r is the shock compression ratio, which is assumed to be equal to 4 (the strong shock limit, ignoring non-linear effects from CR feedback) hereafter.

We then solve the transport equation (2) by imposing the following

boundary conditions:

$$(i) \quad \lim_{x \rightarrow -0} f_i = \lim_{x \rightarrow +0} f_i, \quad (5)$$

$$(ii) \quad \lim_{x \rightarrow -l} f_i = 0, \quad (6)$$

$$(iii) \quad \left| \lim_{x \rightarrow +\infty} f_i \right| < \infty, \quad (7)$$

$$(iv) \quad \left[D_i(p) \frac{\partial f_i}{\partial x} \right]_{x=0}^{x=-0} = \frac{1}{3} (u_+ - u_-) p \frac{\partial f_{i,0}}{\partial p} + u_- Q_i \delta(p - p_0), \quad (8)$$

where condition (i) means that the distribution functions should be continuous across the shock, and condition (ii) means the free escape of CR particles from the outer boundary. Condition (iv) comes from the integration of Eq.(2) across the shock front ($x = 0$), and it yields the differential equation for the distribution function at $x = 0$ with respect to p , $f_{i,0}(p)$. Hereafter we solve Eq.(2) for the relativistic regime, i.e., the kinetic energy per nucleon ε_k is greater than a few GeV/n, so that we can approximate $p \approx A\varepsilon_k/c$.

Following Mertsch & Sarkar (2009) we can solve for the energy distribution function of nuclei i , $N_i(\varepsilon_k) = 4\pi p_i^2 f_i(p)(dp_i/d\varepsilon_k)$ separately in the downstream ($x > 0$) and the upstream ($x < 0$), where we can neglect the second and fifth terms on the right hand side of Eq.(2). In the downstream and upstream, the solutions of Eq.(2) are described respectively as

$$N_i^+ = \sum_{j \geq i} E_{ji} e^{\lambda_j x/2}, \quad (9)$$

$$N_i^- = \sum_{j \geq i} F_{ji} e^{\kappa_j x/2} + G_i, \quad (10)$$

where

$$\lambda_j = \frac{u_+}{D_j} \left(1 - \sqrt{1 + 4D_j \Gamma_j / u_+^2} \right), \quad (11)$$

$$\kappa_j = \frac{u_-}{D_j} \left(1 + \sqrt{1 + 4D_j \Gamma_j / u_-^2} \right), \quad (12)$$

and E_{ji} and F_{ji} are determined recursively as

$$E_{ji} = \frac{-4 \sum_{m \leq j} \Gamma_{m \rightarrow i} E_{jm}}{D_i \lambda_j^2 - 2u_+ \lambda_j - 4\Gamma_i} \quad (\text{for } j > i), \quad (13)$$

$$E_{ii} = N_{i,0} - \sum_{j > i} E_{ji}, \quad (14)$$

$$F_{ji} = \frac{-4 \sum_{m \leq j} \Gamma_{m \rightarrow i} F_{jm}}{D_i \kappa_j^2 - 2u_- \kappa_j - 4\Gamma_i} \quad (\text{for } j > i), \quad (15)$$

$$F_{ii} = \frac{N_{i,0} - \sum_{j > i} F_{ji} (1 - e^{-\kappa_j l/2})}{1 - e^{-\kappa_i l/2}}, \quad (16)$$

$$G_i = N_{i,0} \left(1 - \frac{1}{1 - e^{-\kappa_i l/2}} \right) - \sum_{j > i} F_{ji} \frac{e^{-\kappa_j l/2} - e^{-\kappa_i l/2}}{1 - e^{-\kappa_i l/2}} \quad (17)$$

where $N_{i,0} = 4\pi p_i^2 f_{i,0}(p_i)(dp_i/d\varepsilon_k)$. The differential equation for the distribution function at the shock front $f_{i,0}$ can be derived from the boundary condition (iv) as

$$p \frac{\partial f_{i,0}}{\partial p} = -\frac{3D_i}{2(u_- - u_+)} \left[\left(\frac{\kappa_i}{1 - e^{-\kappa_i l/2}} - \lambda_i \right) f_{i,0} + \sum_{j > i} \left\{ \tilde{F}_{ji} \left(\kappa_j - \frac{1 - e^{-\kappa_j l/2}}{1 - e^{-\kappa_i l/2}} \kappa_i \right) - \tilde{E}_{ji} (\lambda_j - \lambda_i) \right\} \right] + \frac{3u_-}{u_- - u_+} Q_i \delta(p - p_0), \quad (18)$$

where

$$\tilde{E}_{ji} = \frac{E_{ji}}{4\pi p_i^2 (dp_i/d\varepsilon_k)}, \quad (19)$$

$$\tilde{F}_{ji} = \frac{F_{ji}}{4\pi p_i^2 (dp_i/d\varepsilon_k)}. \quad (20)$$

The difference between Mertsch & Sarkar (2009) and this study is the position of the (effective) escape boundary: the former assumes that f_i should damp at $x = -\infty$, while we impose the outer boundary condition $f_i = 0$ at a finite distance, $x = -l$. When the acceleration timescale is much shorter than the spallation timescale (i.e., $\Gamma_i D_i / u_-^2 \ll 1$) and the escape boundary is very far from the shock front (i.e., $e^{-\kappa_i l/2} \ll 1$), this equation is asymptotically identical to Eq. (17) in Mertsch & Sarkar (2009).

We can evaluate the escape flux of CR nuclei from the SNR at $x = -l$ as

$$\begin{aligned} \phi_i(p) &= u_- f_i|_{x=-l} - D_i(p) \left. \frac{\partial f_i}{\partial x} \right|_{x=-l} \\ &= -D_i(p) \sum_{j \geq i} \frac{\kappa_j}{2} \tilde{F}_{ji} e^{-\kappa_j l/2}, \end{aligned} \quad (21)$$

which is the function of time through the size of the escape boundary, l . The energy spectrum of CR particles escaping the SNR per unit time is given by

$$\frac{dN_{\text{esc},i}(\varepsilon_k)}{dt} \simeq 4\pi R_{\text{sh}}^2 \cdot 4\pi \left(\frac{A\varepsilon_k}{c} \right)^2 |\phi_i(p)| \frac{dp_i}{d\varepsilon_k}, \quad (22)$$

where R_{sh} is the radius of the SNR shock.

To understand the nature of the escape flux $\phi_i(p)$, let us assume that the i -nuclei are purely primary (i.e., they are not produced via spallation of heavier nuclei), and that the loss due to spallation is negligible. In this case, the escape flux can be described as

$$-\phi_i(p) = \frac{u_- f_{i,0}(p)}{\exp(u_- l / D_i) - 1}, \quad (23)$$

Here we assume Bohm-type diffusion, in which the mean free path of a charged particle is proportional to its Larmor radius, inside the SNR:

$$D_i(p) = \eta_g \frac{c^2 p}{3ZeB}, \quad (24)$$

where B is the magnetic field strength and η_g is the gyro factor. We can see that the momentum at which the absolute value of the escape flux of the i -nuclei attains its maximum value is given by

$$p = p_{i,m} \equiv \frac{3u_- l Z e B}{\gamma c^2 \eta_g}, \quad (25)$$

and the maximum value of the escape flux is

$$-\phi_i(p_{i,m}) = \frac{u_- f_{i,0}(p_{i,m})}{e^\gamma - 1}, \quad (26)$$

(Caprioli et al. 2009; Ohira et al. 2010). Noting that the distribution function at the shock front behaves as $f_{i,0} \propto p^{-\gamma}$ when $p \ll p_{i,m}$ where $\gamma = 3u_- / (u_- - u_+) = 3r / (r - 1)$, and that $f_{i,0}(p) \propto \exp(-p/p_{i,m})$ when $p \gg p_{i,m}$, the particles accelerated at the SNR shock with momentum $p_{i,m}$ can escape the SNR most efficiently, i.e., $p_{i,m}$ can be regarded as the maximum momentum of the escaping particles.

To evaluate the resulting CR spectra, we need a model for the spatial diffusion coefficient, $D_i(p)$, which in general depends on time because of the evolution of the magnetic field around the shock, and the primary CR injection rate at the shock, Q_i . In the next section,

we describe a phenomenological model to determine these quantities based on analytic formulae of SNR evolution and the observed spectra of Galactic CRs.

2.3 Evolution of SNRs and CR fluxes

Neglecting the back reaction of particle acceleration, the dynamics of the SNR shock can be well described by analytic solutions. When an SNR is surrounded by the ISM or a CSM, the SNR expands freely until it sweeps up a mass comparable to its own mass from the surrounding medium, and afterward the SNR shell is decelerated and expands in a self-similar way. This is so called the Sedov-Taylor phase, and the evolution of the SNR shell radius is determined by the explosion energy of a supernova E_{SN} , the ejecta mass M_{ej} , and the number density of the ambient medium n . In the case with the uniform ISM, the SNR shell radius is given by

$$R_{\text{sh}} = R_{\text{S}} \left(\frac{t}{t_{\text{S}}} \right)^{2/5} \quad (27)$$

where R_{S} and t_{S} are the Sedov radius and Sedov time, respectively, and they are given by

$$R_{\text{S}} = 4.59 \text{ pc} \left(\frac{M_{\text{ej}}}{1M_{\odot}} \right)^{1/3} \left(\frac{n}{0.1 \text{ cm}^{-3}} \right)^{-1/3}, \quad (28)$$

$$t_{\text{S}} = 450 \text{ yr} \left(\frac{E_{\text{SN}}}{10^{51} \text{ erg}} \right)^{-1/2} \left(\frac{M_{\text{ej}}}{1M_{\odot}} \right)^{5/6} \left(\frac{n}{0.1 \text{ cm}^{-3}} \right)^{-1/3} \quad (29)$$

. While in the case that the ambient density profile is wind-like (i.e. $n \propto r^{-2}$), the SNR shell radius is given by

$$R_{\text{sh}} = R_{\text{S}} \left(\frac{t}{t_{\text{S}}} \right)^{2/3} \quad (30)$$

where

$$R_{\text{S}} = 1.26 \text{ pc} \left(\frac{M_{\text{ej}}}{1M_{\odot}} \right) \left(\frac{\dot{M}}{10^{-3} M_{\odot} \text{ yr}^{-1}} \right)^{-1} \left(\frac{v_w}{100 \text{ km s}^{-1}} \right), \quad (31)$$

$$t_{\text{S}} = 178 \text{ yr} \left(\frac{E_{\text{SN}}}{10^{51} \text{ erg}} \right)^{-1/2} \left(\frac{M_{\text{ej}}}{1M_{\odot}} \right)^{3/2} \left(\frac{\dot{M}}{10^{-3} M_{\odot} \text{ yr}^{-1}} \right)^{-1} \\ \times \left(\frac{v_w}{100 \text{ km s}^{-1}} \right), \quad (32)$$

where \dot{M} and v_w are the mass loss rate and wind velocity, respectively. Here we use the density profile for a steady wind, i.e., $n = \dot{M} / (4\pi m_p v_w r^2)$.

We here adopt a phenomenological model proposed by Gabici et al. (2009) (see also Ohira et al. 2010), which is based on the assumption that Galactic SNRs are responsible for CRs with energy below the knee ($\sim 10^{15.5}$ eV). In this model it is assumed that the maximum momentum of a CR particle $p_{i,m}$ accelerated at the SNR is limited by its escape during the Sedov-Taylor phase, and that the maximum energy of an escaping particle, $\sim c p_{i,m}$, at the beginning of the Sedov phase is equal to the knee energy ($\sim 10^{15.5}$ eV). Using a variable χ to describe the evolution of an SNR (e.g., the SNR's age, the shock radius of an SNR, etc.), we assume that the maximum momentum of an escaping CR particle decreases with time as $p_{i,m} \propto \chi^{-\alpha}$, and that the spectrum of CRs accelerated at the SNR is proportional to $\chi^{\beta} p^{-s}$ (i.e., CRs inside the SNR have a power-law spectrum with index of s and their total number increases with time). One can then see that the spectrum of CRs escaping the SNR is proportional to $p^{-s+\beta/\alpha}$. This means that if α and β are positive (i.e., the maximum momentum decreases and the total number of accelerated CRs increases with time), the spectrum of escaping CRs

become steeper than that inside the SNR. Here α and β are the phenomenological parameters that are determined so that the resulting CR spectra are consistent with observations. Following Ohira et al. (2010), we hereafter adopt R_{sh} as χ , and fix the parameters as $\alpha = 6.5$ and $\beta = 2.1$. Actually, with these parameters, the maximum energy of escaping CRs evolves from the knee energy at the beginning of the self-similar phase to 1 GeV at the end of the Sedov phase, when the radius of the SNR shell becomes 10 times larger than R_{S} , and the spectral index of escaping primary CRs would be similar to what is inferred from observations, assuming that the diffusion coefficient in the ISM, $D_{\text{ISM}}(R)$, is proportional to a power of rigidity, R .

One can determine the diffusion coefficient and the normalization factor of the escaping CR flux in the following way. First, the time dependence of $p_{i,m}$ ($\propto \chi^{-\alpha}$) is related to the evolution of the diffusion coefficient, which depends on the amplification and decay of magnetic field and the turbulence around the shock (Ptuskin & Zirakashvili 2003, 2005; Yan et al. 2012). Assuming the Bohm diffusion inside the SNR, one can determine the evolution of the diffusion coefficient in the SNR using the relation in Eq.(25). Assuming $l \propto R_{\text{sh}}$, we can describe the evolution of the diffusion coefficient at a specific momentum as $\propto \chi^{\alpha-1/2}$ in the case with uniform ISM, while $\propto \chi^{\alpha+1/2}$ in the case with the wind-like ambient density profile. Second, the normalization factor of the spectrum of CRs accelerated at the SNR ($\propto \chi^{\beta}$) is related to the CR injection rate at the shock, Q_i . If we assume that Q_i evolves with time as $\propto \chi^{\beta'}$ where β' is a constant, since the escaping CR spectrum per unit time is expressed as Eq.(22), where $\phi(p)$ is proportional to $u_{\text{sh}} f_{i,0}$, one can see that the time-integrated spectrum of escaping CRs would be

$$\int dt \frac{dN_{\text{esc},i}}{dt} \propto \chi^{\beta'+3} p_{i,m}^{\gamma-2} \\ \propto p^{-(\gamma-2)-\frac{\beta'+3}{\alpha}}, \quad (33)$$

where we use $p_{i,m} \propto \chi^{-\alpha}$. Considering that the power-law index of the on-site CR spectrum is $\sim \gamma - 2$, we can see how Q_i should increase with time as

$$\beta' = \beta - 3. \quad (34)$$

2.4 Observed CR Spectra from a Local Single SNR

In this study, we try to explain the observed CR spectral hardening above ~ 200 GV by introducing a single local SNR surrounded by the ISM or a dense CSM. The propagation of CR particles in the ISM can be described by the diffusion equation,

$$\frac{\partial}{\partial t} f_{i,\text{ISM}}(r, p, t) = D_{\text{ISM}}(p) \nabla^2 f_{i,\text{ISM}}(r, p, t) + q_i(r, p, t), \quad (35)$$

where $f_{i,\text{ISM}}(r, p, t)$ is the distribution function of CR particles in the ISM at a distance r from the source and the time t , with momentum p , and $q_i(r, p, t)$ is the CR injection rate from the source, which is located at $r = 0$ (i.e., $q_i \propto \delta(r)$). In our case, this diffusion equation can be solved as

$$f_{i,\text{ISM}}(r, p, t) = \int_0^t dt' \frac{4\pi R_{\text{sh}}(t')^2 p^2 |\phi_i(p)|}{(4\pi D_{\text{ISM}} t')^{3/2}} \exp\left(-\frac{r^2}{4D_{\text{ISM}} t'}\right). \quad (36)$$

. The observed spectra can then be obtained by summing this distribution function and the background flux due to the myriad of sources in the Galaxy.

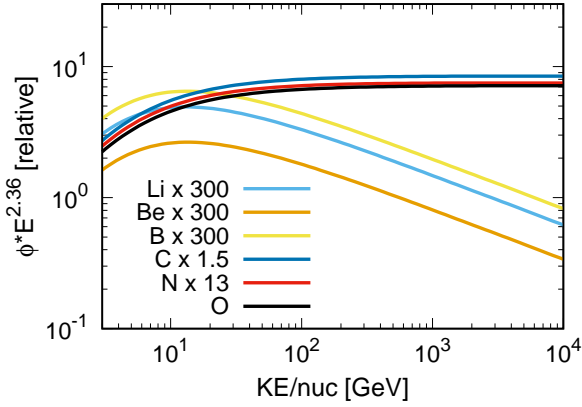


Figure 1. Time-integrated energy spectra of CR nuclei escaping the SNR surrounded by a uniform interstellar medium. The ambient density is assumed to be 0.1 cm^{-3} .

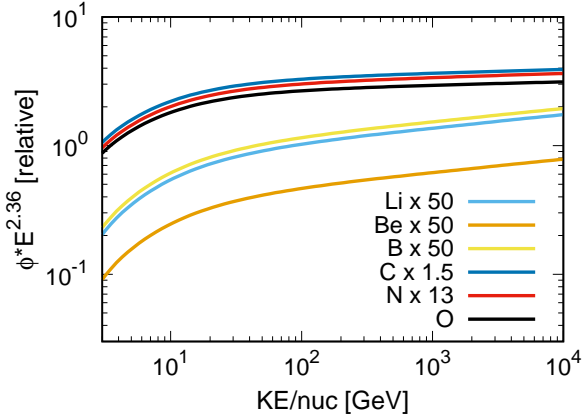


Figure 2. Time-integrated energy spectra of CR nuclei escaping the SNR surrounded by a wind-like circumstellar medium. The mass loss rate and wind velocity are assumed to be $3 \times 10^{-3} M_{\odot} \text{ yr}^{-1}$ and 100 km s^{-1} , respectively.

3 RESULTS AND DISCUSSION

3.1 Time integrated energy spectra of CR nuclei escaping the SNR

Fig. 1 depicts the time-integrated spectra of CRs that have escaped the SNR surrounded by a uniform ISM whose density is 0.1 cm^{-3} , and Fig. 2 depicts those escaped the SNR surrounded by a wind-like medium whose mass loss rate and velocity are $3 \times 10^{-3} M_{\odot} \text{ yr}^{-1}$ and 100 km s^{-1} , respectively. In both cases, the explosion energy and ejecta mass of the supernova are assumed to be 10^{51} erg and $3 M_{\odot}$ respectively, and the elemental abundance in CRs are assumed to be identical to that of the background CRs. In the former case, the spectra of secondary nuclei (lithium, beryllium, and boron) are softer than those of the primary nuclei (carbon and oxygen), while in the latter case the spectra of secondary nuclei are a bit harder than those of primary nuclei. These spectral features and the difference between two cases can be interpreted in the following way. Since the secondary CR nuclei escaping the SNR are produced by the spallation of primary CR nuclei being accelerated at the shock, the number of CR particles escaping the SNR per unit time is proportional to $u_{-} f_{\text{pr}} n_{\text{amb}} t_{\text{int}}$, where f_{pr} is the distribution function of their parent nuclei accelerated at the shock (χ^{β}), n_{amb} is the density of the am-

bient gas (constant, or $\propto \chi^{-2}$), and t_{int} is the time during which their parent nuclei interact with the ambient gas before escape. Especially, in the escape-limited regime, t_{int} is equal to their acceleration time in the SNR, $\sim D_i/u_{-}^2$. Since we are assuming Bohm diffusion in the SNR, $D_i \propto p$, the intrinsic spectral index of secondary nuclei inside the SNR would be $s - 1$. On the other hand, the normalization factor of the secondary CR flux evolves with time as $\propto D_i/u_{-}^2 \cdot \chi^{\beta}$ in the case of a uniform ISM and $\propto D_i/u_{-}^2 \cdot \chi^{-2} \cdot \chi^{\beta}$ in the case of a wind-like ambient medium. Taking into account the time-dependence of the shell expansion velocity ($u_{-} \propto \chi^{-3/2}$ in the case of uniform ISM and $u_{-} \propto \chi^{-1/2}$ in the case with the wind-like ambient medium) and the diffusion coefficient (see the previous section), we can evaluate the spectral index of the distribution function of secondary CR nuclei escaping the SNR per unit time as

$$(s - 1) + \frac{-3/2 + \beta + (\alpha + 5/2)}{\alpha} = s + \frac{\beta + 1}{\alpha}, \quad (37)$$

in the case of uniform ISM, and

$$(s - 1) + \frac{-1/2 + \beta - 2 + (\alpha + 3/2)}{\alpha} = s + \frac{\beta - 1}{\alpha}, \quad (38)$$

in the case of wind-like ambient medium. Now we can see that in the former case the spectrum of secondary nuclei is softer, while in the latter case it is harder compared to that of the primary nuclei. This difference is caused mainly by the difference in the density profile of the ambient medium. Generally, the CR particles with higher energy would escape the SNR earlier, so the time for primary CRs with higher energy to produce secondary CRs due to the interaction with ambient matter would be shorter. This makes the number of escaping secondary CRs with higher energy smaller when the ambient matter distribution is uniform. By contrast, when the SNR is surrounded by a wind-like CSM, the primary CRs escaping into the ISM earlier can interact with larger amount of matter than those escaping later, and then the number of secondary CRs produced by them is enhanced. As a result, the energy spectrum of secondary CRs escaping the SNR would be harder than that of primary CRs. Note that this spectral hardening of secondary nuclei is essentially different from what have been studied in Mertsch & Sarkar (2009) and Mertsch & Sarkar (2014), in that they discussed the acceleration of secondary CRs produced inside the SNR assuming that the maximum energy of accelerated CRs is limited by the age of the SNR. In this scenario, the primary CRs with higher energy can interact with ambient medium longer and produce more secondary CRs than those with lower energy. However, they did not take into account the energy-dependent escape of primary and secondary CRs, or the non-uniform distribution of ambient medium, both of which have been implied by recent observations of SNRs and SNe.

According to the recent measurements of secondary CR nuclei by AMS-02 (Aguilar et al. 2018), the spectra of lithium, beryllium, and boron are hardened at $\sim 200 \text{ GV}$ as has been observed for primary CR nuclei, but they harden more than the primaries. To account for such a feature, we will introduce the CR contribution from a past local SN. In this context, the case with a wind-like CSM, which can make the spectra of secondary CRs harder, is more relevant. In the following discussions, therefore, we will show results for the wind-like CSM case only. In addition to the elements shown in Figure 2, we also show the spectra of protons and helium nuclei expected from the SNR in the next section.

3.2 Observed spectra of CR nuclei

In our scenario, we assume that the flux of CR nuclei observed by AMS-02 is a superposition of two components: one is from a

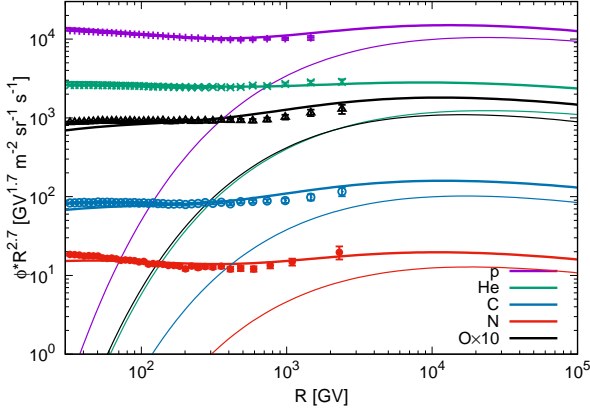


Figure 3. Comparisons of our model spectra of CR oxygen, nitrogen, and carbon with AMS-02 data. The contributions from our hypothetical past CSM-interacting SN are also shown by thin lines.

age	1.6×10^5 year
distance	1.6 kpc
total energy	10^{51} erg
ejecta mass	$3 M_{\odot}$
mass loss rate	$2.5 \times 10^{-3} M_{\odot} \text{ yr}^{-1}$
wind velocity	100 km s $^{-1}$

Table 1. Properties of the past local SN we introduced to explain the AMS-02 data.

local SNR with a wind-like CSM that is supposed to reproduce the hardenings observed in the CR nuclei spectra at ~ 200 GV, and the other is the background flux due to average SNRs without dense CSM (i.e., these SNRs do not produce hard secondary CRs efficiently inside themselves). As for the first component, we can calculate its flux using Eq.(36), choosing the parameters such as the distance and age of the SNR, total CR energy, CSM properties, abundance ratio in CRs, etc. On the other hand, the background flux of i -th nuclei N_i is given recursively by

$$N_i(\varepsilon_k) = \frac{\sum_{i < j} \Gamma_{j \rightarrow i} N_j(\varepsilon_k) + \mathcal{R} N_{\text{esc},i}(\varepsilon_k)}{1/\tau_{\text{esc},i}(\varepsilon_k) + \Gamma_i}, \quad (39)$$

where $\mathcal{R} \approx 0.03 \text{ yr}^{-1}$ is the Galactic SN rate and $\tau_{\text{esc},i}(\varepsilon_k)$ is the timescale for an i -th nucleus with kinetic energy per nucleon of ε_k to escape from the Galaxy, which is modeled using an expression of D_{ISM} ,

$$\tau_{\text{esc},i} \approx \frac{H^2}{D_{\text{ISM}}(A_i \varepsilon_k / Z_i)}, \quad (40)$$

where $H \approx 3$ kpc is half the thickness of the Galactic halo. In our calculation, we assume the diffusion coefficient in the ISM as $D_{\text{ISM}}(R) = D_0 (R/1 \text{ GV})^{0.45}$ where $D_0 = 2 \times 10^{28} \text{ cm}^2 \text{ s}^{-1}$.

Figure 3 depicts the observed spectra of proton, helium, carbon, nitrogen, and oxygen nuclei, and Figure 4 depicts the observed spectra of lithium, beryllium, and boron nuclei as functions of rigidity reported by AMS-02, fitted by our model. Figure 5 depicts the predicted ratios of lithium to carbon, beryllium to carbon, and boron to carbon in the observed CRs as functions of rigidity compared with

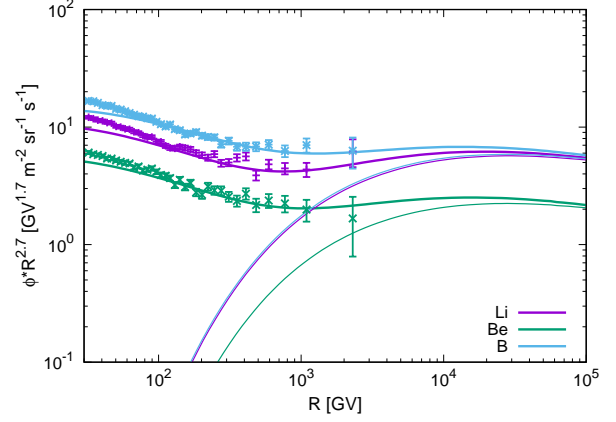


Figure 4. Comparisons of our model spectra of CR boron, beryllium, and lithium with AMS-02 data. The contributions from our hypothetical past CSM-interacting SN are also shown by thin lines.

the ratios reported by AMS-02. In making these plots, we assume a local SNR surrounded by dense wind-like CSM with parameters summarized in Table 1. As for the elemental abundance in CRs, we assume that the fractions of carbon, nitrogen, and oxygen are three times as much as those in the background CRs. We can see that the hard component appearing above ~ 200 GV in each spectrum is well explained by introducing this local SNR. The important point here is that we can fit not only the spectra of primary CRs (i.e., oxygen and carbon) but also that of secondary CRs (i.e., lithium, beryllium and boron) by taking into account the production, acceleration, and escape of secondary CRs inside a local SNR surrounded by a dense CSM. Another remarkable thing is that our model can be tested by the secondary to primary ratios at rigidity of $\gtrsim 1$ TeV: within our model, they are predicted to show rising or flattening with rigidity. Such a feature is never expected as long as we consider the ISM propagation effects as the origin of spectral hardening of CR nuclei. As shown in Section 3.1, the energy spectra of secondary CR nuclei escaping a SNR surrounded by wind-like medium would be harder than those of the primary CR nuclei. Since the observed CR spectra above ~ 200 GV are dominated by the contribution from a hypothetical SNR in our model, the predicted secondary-to-primary ratios in this rigidity range would reflect the hardening of secondary CRs escaping the SNR. The secondary-to-primary ratios above ~ 1 TeV will be explored by future experiments such as AMS-100 (Schael et al. 2019), which will provide a critical test for the existence of such a local SNR with dense wind-like CSM.

3.3 Origin of the local SNR with a dense CSM

While it is beyond the scope of this study to discuss in depth about the progenitor nature and detailed mass loss mechanism of the proposed local SNR, it is instructive to briefly account on its possible origin, and the feasibility of invoking such a local source without violating current observations. There exists a few possible scenarios for an enhanced mass loss rate during a certain period prior to core-collapse, such as giant eruptions at the envelope, envelope stripping in a binary system by Roche-lobe overflow (RLOF) to a companion star and a possible common envelope phase, and so on (see, e.g., Smith 2014). The hypothetical close-by SNR invoked here in particular can possibly be the result of a past SN of type Ib/c, originating from the explosion of a Wolf-Rayet (WR) star in a close binary system (e.g., Yoon et al. 2010; Dessart et al. 2012, and reference therein). For ex-

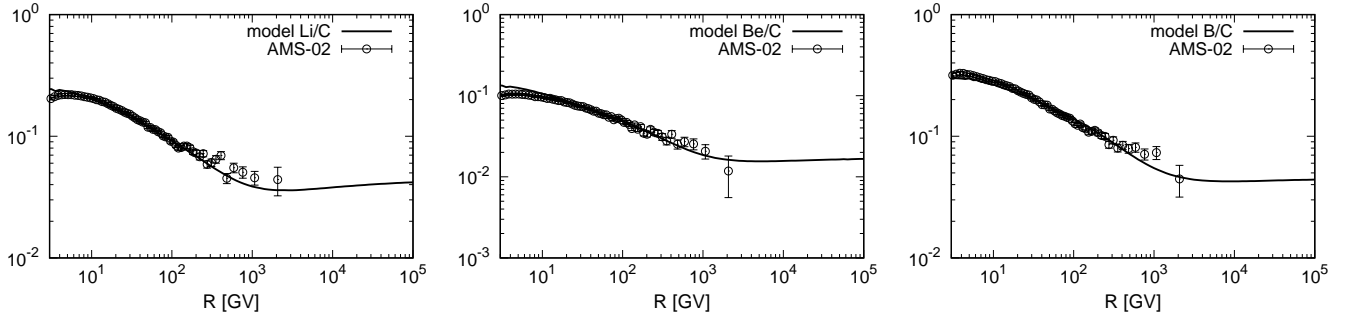


Figure 5. Li/C (left), Be/C (center), and B/C (right) ratios in the observed CRs reported by AMS-02 along with our model predictions.

ample, a RLOF phase that lasts for $\sim 10^4$ yrs with a mass loss rate of $\sim 10^{-3}$ Msun/yr and a velocity ~ 100 km/s can result in a dense CSM extending up to a radius $R_w \sim 1$ pc. Assuming an ejecta mass of $3M_\odot$ typical for SN Ib/c, and for simplicity a r^{-2} density profile for the CSM structure and the mass loss parameters in Table 1, the Sedov radius R_S of the SNR is about 0.1 pc.¹ This is much smaller than R_w , and the transition to Sedov phase happened at an age of roughly 10 yrs old. Therefore, the escape of the highest energy CRs must have occurred when the SNR blastwave was still in the midst of interacting with the dense CSM material, which is consistent with our picture above.

On the other hand, the required chemical enhancement of heavy metal abundances in the CRs produced by this local accelerator is also consistent with a stripped envelope SN origin, in that the CSM in the vicinity of the ejecta of a type Ib/c progenitor is expected to be rich in metals in comparison to that around a SN IIP from the explosion of a red super-giant star (e.g., Yoon 2015). The blast wave colliding with this metal-rich CSM shell in the early phase after SN should then be able to accelerate these heavy ions to high energies². This interaction between the blastwave and a chemically-enriched CSM shell has been suggested by recent observations of type Ibn SNe (e.g., see review in Smith 2017), or even the hypothetical type Icn that may be detected in the future. Meanwhile, at a current age of 1.6×10^5 yrs, the shock should have long died out already due to radiative loss, and the SNR should have merged with and become indistinguishable from the surrounding ISM, rendering it invisible in various wavebands at a distance > 1 kpc. A more detailed model for the evolution and broadband emission of such a stripped-envelope SNR interacting with a dense CSM using a method similar to Yasuda & Lee (2019) will be presented in a follow-up paper (Matsuoka et al., in preparation).

4 SUMMARY

In this paper, we investigated the effect of the production of secondary CR nuclei at supernova remnants by the diffusive shock acceleration mechanism on the CR population measured near the Earth using an

¹ We are ignoring any anisotropy and episodic history of the mass loss from the progenitor here.

² We note that ejecta of SN Ib/c can reach trans-relativistic velocities right after explosions, for which particle acceleration at the shock can be modelled self-consistently using methods such as Monte-Carlo simulations (e.g., Ellison et al. 2013; Warren et al. 2015). A more accurate approach with treatment of DSA at trans-relativistic shocks will be done in a future work.

analytic approach. By including nuclear spallation effects and acceleration locally at the acceleration sites, we predicted the spectra of the accelerated ions escaping from the SNR shocks. Our results show that the secondary CR nuclei escaping the SNR have a softer spectral index compared to the primary CRs when the SNR is surrounded by uniform ISM, while they have a harder spectral index when they are surrounded by the CSM with a wind-like density profile. We show that, by introducing a past and relatively close-by SN event surrounded by a wind-like CSM, the current CR measurements including the spectral hardening recently discovered above a few 100 GV in ion species up to oxygen can be successfully reproduced. We suggest that this past local accelerator can be a SN of type Ib/c with its progenitor enclosed by a CSM from pre-SN mass loss highly enriched in heavy metals. Our model also predicts a characteristic spectral flattening of CR secondary-to-primary ratios, such as Li/C, Be/C and so on, above a rigidity ~ 1 TV. Future CR measurements by next-generation experiments such as AMS-100 with an extended high energy range will put this to the test.

ACKNOWLEDGEMENT

N.K. acknowledges support by the Hakubi project at Kyoto University. S.H.L. acknowledges support by JSPS Grant No. JP19K03913 and the World Premier International Research Center Initiative (WPI), MEXT, Japan.

REFERENCES

- Adriani O., et al., 2009, *Nature*, **458**, 607
 Adriani O., et al., 2011, *Science*, **332**, 69
 Aguilar M., et al., 2013, *Physical Review Letters*, **110**, 141102
 Aguilar M., et al., 2015a, *Physical Review Letters*, **114**, 171103
 Aguilar M., et al., 2015b, *Physical Review Letters*, **115**, 211101
 Aguilar M., et al., 2016a, *Physical Review Letters*, **117**, 091103
 Aguilar M., et al., 2016b, *Physical Review Letters*, **117**, 231102
 Aguilar M., et al., 2017, *Phys. Rev. Lett.*, **119**, 251101
 Aguilar M., et al., 2018, *Phys. Rev. Lett.*, **120**, 021101
 Ahlers M., Mertsch P., Sarkar S., 2009, *Phys. Rev. D*, **80**, 123017
 Ahn H. S., et al., 2010, *ApJ*, **714**, L89
 Bell A. R., 1978, *MNRAS*, **182**, 147
 Bell A. R., Schure K. M., Reville B., Giacinti G., 2013, *MNRAS*, **431**, 415
 Blandford R., Eichler D., 1987, *Phys. Rep.*, **154**, 1
 Boschini M. J., et al., 2020, *ApJ*, **889**, 167
 Bresci V., Amato E., Blasi P., Morlino G., 2019, *MNRAS*, **488**, 2068
 Caprioli D., Blasi P., Amato E., 2009, *MNRAS*, **396**, 2065

- Caprioli D., Kang H., Vladimirov A. E., Jones T. W., 2010, *MNRAS*, **407**, 1773
- Cholis I., Hooper D., 2014, *Phys. Rev. D*, **89**, 043013
- Cowsik R., Burch B., 2010, *Phys. Rev. D*, **82**, 023009
- Cowsik R., Madziwa-Nussinov T., 2016, *ApJ*, **827**, 119
- Cowsik R., Burch B., Madziwa-Nussinov T., 2014, *ApJ*, **786**, 124
- Cristofari P., Renaud M., Marcowith A., Dwarkadas V. V., Tatischeff V., 2020, *MNRAS*, **494**, 2760
- Dessart L., Hillier D. J., Li C., Woosley S., 2012, *MNRAS*, **424**, 2139
- Drury L. O., 2011, *MNRAS*, **415**, 1807
- Ellison D. C., Warren D. C., Bykov A. M., 2013, *The Astrophysical Journal*, **776**, 46
- Gabici S., Aharonian F. A., Casanova S., 2009, *MNRAS*, **396**, 1629
- Kachelrieß M., Ostapchenko S., 2013, *Phys. Rev. D*, **87**, 047301
- Kawanaka N., Yanagita S., 2018, *Phys. Rev. Lett.*, **120**, 041103
- Kawanaka N., Ioka K., Ohira Y., Kashiyama K., 2011, *ApJ*, **729**, 93
- Kolmogorov A., 1941, *Akademiia Nauk SSSR Doklady*, **30**, 301
- Lucek S. G., Bell A. R., 2000, *MNRAS*, **314**, 65
- Matsuoka T., Maeda K., 2020, *ApJ*, **898**, 158
- Matsuoka T., Maeda K., Lee S.-H., Yasuda H., 2019, *ApJ*, **885**, 41
- Mertsch P., Sarkar S., 2009, *Physical Review Letters*, **103**, 081104
- Mertsch P., Sarkar S., 2014, *Phys. Rev. D*, **90**, 061301
- Mertsch P., Vittino A., Sarkar S., 2020, arXiv e-prints, p. [arXiv:2012.12853](https://arxiv.org/abs/2012.12853)
- Moriya T. J., Maeda K., Taddia F., Sollerman J., Blinnikov S. I., Sorokina E. I., 2014, *MNRAS*, **439**, 2917
- Murase K., Franckowiak A., Maeda K., Margutti R., Beacom J. F., 2019, *ApJ*, **874**, 80
- Niu J.-S., 2020, arXiv e-prints, p. [arXiv:2009.00884](https://arxiv.org/abs/2009.00884)
- Ohira Y., Ioka K., 2011, *ApJ*, **729**, L13
- Ohira Y., Murase K., Yamazaki R., 2010, *A&A*, **513**, A17
- Ohira Y., Murase K., Yamazaki R., 2011, *MNRAS*, **410**, 1577
- Ohira Y., Yamazaki R., Kawanaka N., Ioka K., 2012, *MNRAS*, **427**, 91
- Ohira Y., Kawanaka N., Ioka K., 2016, *Phys. Rev. D*, **93**, 083001
- Ptuskin V. S., Zirakashvili V. N., 2003, *A&A*, **403**, 1
- Ptuskin V. S., Zirakashvili V. N., 2005, *A&A*, **429**, 755
- Reville B., Kirk J. G., Duffy P., 2009, *ApJ*, **694**, 951
- Schael S., et al., 2019, *Nuclear Instruments and Methods in Physics Research A*, **944**, 162561
- Smith N., 2014, *Annual Review of Astronomy and Astrophysics*, **52**, 487
- Smith N., 2017, *Interacting Supernovae: Types II_n and Ib_n*. p. 403, [doi:10.1007/978-3-319-21846-5_38](https://doi.org/10.1007/978-3-319-21846-5_38)
- Tomassetti N., 2012, *ApJ*, **752**, L13
- Tomassetti N., 2015, *Phys. Rev. D*, **92**, 081301
- Wang K., Huang T.-Q., Li Z., 2019, *ApJ*, **872**, 157
- Warren D. C., Ellison D. C., Bykov A. M., Lee S.-H., 2015, *MNRAS*, **452**, 431
- Yan H., Lazarian A., Schlickeiser R., 2012, *ApJ*, **745**, 140
- Yasuda H., Lee S.-H., 2019, *ApJ*, **876**, 27
- Yoon S.-C., 2015, *Publications of the Astronomical Society of Australia*, **32**, e015
- Yoon S. C., Woosley S. E., Langer N., 2010, *ApJ*, **725**, 940
- Yuan Q., Zhu C.-R., Bi X.-J., Wei D.-M., 2020, *J. Cosmology Astropart. Phys.*, **2020**, 027
- Zirakashvili V. N., Ptuskin V. S., 2008, *ApJ*, **678**, 939